Lux junior 2023

16. Internationales Forum für den lichttechnischen Nachwuchs
Ilmenau, 23. – 25. Juni 2023
DOI (proceedings): 10.22032/dbt.55787

DOI: 10.22032/dbt.58587

Lab-on-chip Projection System for Fluorescence based Medical Analysis

Oindrila Ghosh[1,2], Jan Müller[1,2], Ingo Ramsteiner[2], Reinhold Fieß[2], Cornelius Neumann[1]

[1]Karlsruhe Institute of Technology, [2]Robert Bosch GmbH

fixed-term.Oindrila.Ghosh@de.bosch.com, jan.mueller9@de.bosch.com

Abstract

The aim of this research project is to implement a novel concept of using a scanning projection system for exciting fluorescence in lab-on-chip devices. While scanning projectors are state of the art in display applications, this use case imposes a set of specific requirements not fulfilled by commercial devices. One advantage in the lab-on-chip setting is increased flexibility in the design of disposables.

To implement the final goal, the theoretical feasibility of the optical system is estimated, followed by simulation of the entire setup in Zemax OpticStudio and finally building up the working prototype of the projection system in the lab as a proof of concept, to compare the experimental findings with the simulation results.

Index Terms: Laser phosphor, scanning projection system, lab-on-chip

1 Introduction

Fluorescence-based detection systems are used in numerous life-science applications, such as immunoassays, tissue staining, cytometry real-time quantitative Polymerase Chain Reaction analysis. The common idea in any of these applications is to make some biomolecular signature or reaction visible, which is not accessible to direct spectroscopy. To this end, special biomolecules that interact in a key-lock manner with molecules (e.g., nucleotide sequences or antibodies) in the sample are functionalized with particular dye molecules. Their fluorescence can be measured and tells us thereby indirectly about molecular properties of the sample.

This paper implements the idea of using a scanning projection system for exciting fluorescence in any of these applications.

2 Motivation

A projector-based illumination system has several advantages a medtech device could benefit from. Mainly, the freedom in distributing the light budget to any part of the

projection area gives great flexibility to either locally enhance intensities or change areas of interest which reduces stray light. It also offers high flexibility in the design of disposables such as lab-on-chip cartridges.

While there are several established projector systems for display purposes, these are typically based on laser diodes. For lab on chip applications, the latter are not suitable for several reasons, the most notable and trivial being the limited availability at custom wavelengths. Therefore, we explore the use of phosphor converted light sources, which makes designing such a projector challenging for etendue reasons.

3 Etendue Calculations

The etendue of an optical system describes the ability to collect a certain fraction of luminous flux from a finite light source. The etendue G of a system is calculated by the equation, $G = \pi S(NA)^2$ where S is the finite area of the light source from which the system can accept luminous flux, and NA is the corresponding numerical aperture. The total luminous flux of a Lambertian emitter is given by $\phi_{source} = \pi A_s L_s$ where A_s is the total area of the light source that emits light, and L_s is the luminance.

The maximum flux which the optical system can accept is given by $\phi_{system} = G\, L_s$.

This equation shows that the flux output is etendue limited and can only be increased by increasing the luminance of the light source. [1]

The beam parameter product of a laser beam which can be described as Gaussian beam, see figure 1, is given as $BPP = w_0 \cdot \Theta_{\mathrm{div}}$, where w_0 represents the beam waist and Θ_{div} represents the beam divergence half-angle.

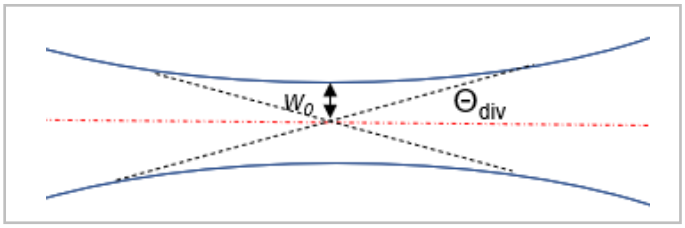

Figure 1: Gaussian beam with beam waist w_0 and divergence Θ_{div}

4 Key Elements

Laser-pumped phosphor light source: Since a projection system, is an etendue-limited optical setup, a source which provides high luminance/radiance output is the best option. Here, a light source from Kyocera SLD Laser is used which is consists of a phosphor converted laser packaged as surface mount device (SMD). The light source emits a broad white spectrum with a luminous flux of 500 lumens (lm). It has a luminance value > 1000 cd/mm2. It consists of a combination of blue laser and yellow phosphor [6].

Scanning mechanical mirror: To scan the sample plane, the Optotune fast-steering mechanical mirror is used. This mirror allows 2D beam deflections of ± 50˚ in both

directions. It has a compact structure with a clear aperture of 15 mm and offers real-time position feedback. By controlling the amplitude of the input current, the deflection angle of the mirror can be monitored as per requirement of the scanning area. [3]

Sample Plane: The system is designed to illuminate, partly or entirely, a sample plane observed by a camera. In a typical example, we aim to illuminate one 5x5 mm^2 area on this plane at a time. The sample plane area corresponding to the camera FoV is bigger than this illuminated area.

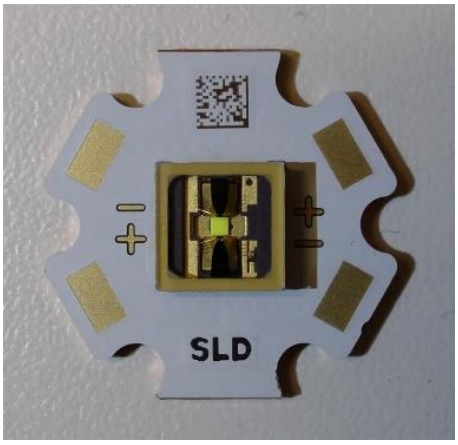

Figure 2 (a) Kyocera SLD element

(b) Optotune scanning mirror

5 System Design

5.1 General Structure

This optical system consists of a light source (the SLD module), a collimation path, an interference filter, a scanning unit followed by a focusing unit that results in a focused spot on the sample plane.

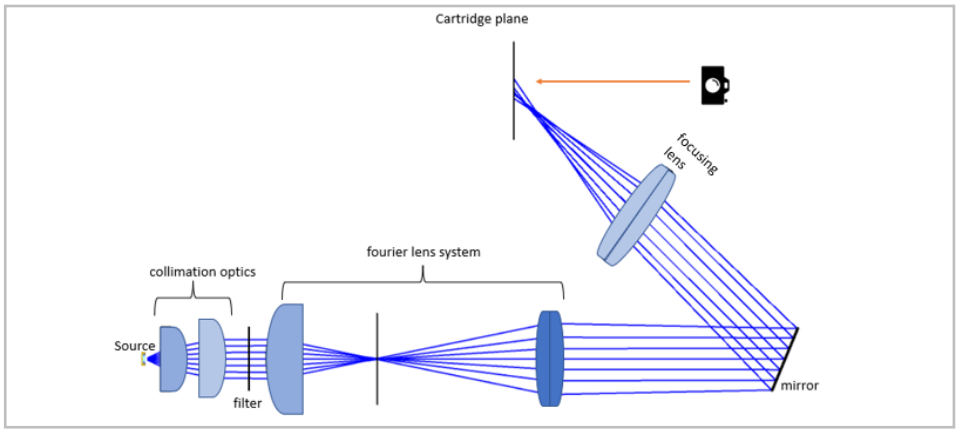

Figure 3: Sketch of the optical system

5.2 Scanning Projection System

In this work, a flying-spot scanning projection system is designed. A flying-spot scanner mainly consists of at least two components: a light source and a deflection unit which scans over an area at a rate higher than human eye can perceive and creates an image.

Based on their working principle, projection systems can be subdivided into two categories: The system of the first type scans the whole field of view, and the light source is modulated to create the desired illumination pattern on the screen. The system of the second type scans only a part of the whole field of view and light source is kept on throughout the scanning period.

The second type of scanning projection system is chosen here since it is evaluated as a more convenient option. In the case of the first kind of scanner, a fraction of the through power of the light source is lost (when then the source is not turned on) and decay time of the phosphor elements limits the rate at which the light source can be modulated.

5.3 Theoretical Feasibility

Alongside with overcoming the field of view limitation, a certain minimum irradiance value and resolution of the scanning spot on the sample plane, is to be maintained for the system to be fully efficient.

The theoretical limit of the system is calculated using the beam parameter product. All assumption describing the optical system are summarized in table 1.

Table 1: Assumptions for the BPP calculation.

Parameter name	symbol	Value
Spot diameter on sample plane	w_{final_spot}	1 mm
Scanning mirror aperture	w_{mirror}	15 mm
Example area on sample (to be scanned at a time)	A_{sample}	25 mm^2
Approximate distance between scanning mirror and sample plane	D	85 mm
Source diameter	w_{source}	0.25 mm
Radiant flux of the source	P_s	1.4 W
Fraction of light transmitted by the spectral filter	η_{filter}	10 %

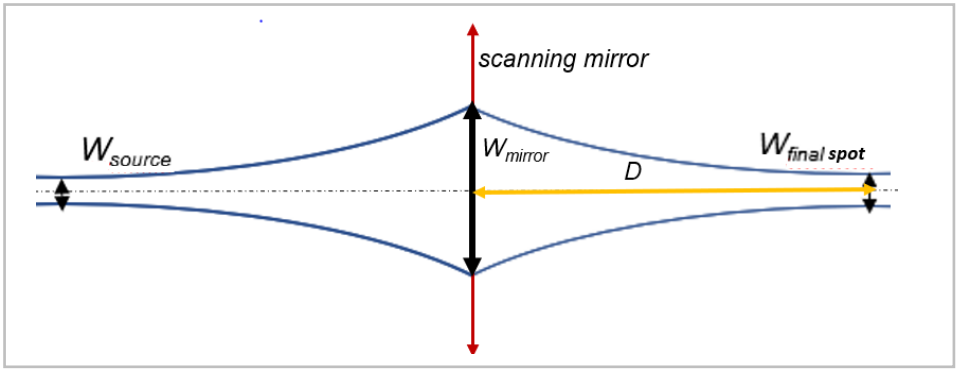

Figure 4: Calculation reference diagram

The divergence of the final spot Θ_{final_spot} is given by equation (1).

$$\Theta_{final\_spot} = \tan^{-1}\left(\frac{w_{mirror} - w_{final\_spot}}{2 \cdot D}\right) = 4.71° \quad (1)$$

$$\Theta_{source} \cdot w_{source} = \Theta_{final\_spot} \cdot w_{final\_spot} \quad (2)$$

The BPP is constant, hence equation (2) is valid. Here, Θ_{source} is the opening angle of the source which can be used from the optical system.

Combining equation (1) and (2), the divergence of the source can be calculated and equals to $\Theta_{source} = 18.8°$ for the given assumptions in table 1. Having the accepted opening angle, the fraction of the source emission cone angle which is used by the optical system can be calculated. To ease the calculation, an Lambertian emitter is assumed whose fraction of flux in a cone angle is given by the sinus of that cone angle. Therefore, the usage efficiency of light from the source η_{source} is given by

$$\eta_{source} = \sin(\Theta_{source}) \quad (3)$$

Which leads to $\eta_{source} = 32.3\%$

To calculate the irradiance E_{sample}, the total through power on the sample plane is divided by A_{sample}:

$$E_{sample} = \frac{P_{source} \cdot \eta_{source} \cdot \eta_{filter}}{A_{sample}} \quad (4)$$

The calculation is made assuming that there is no additional focusing lens after the scanning mirror and still the value calculated using Eq. (4) for the irradiance on the sample $E_{sample} = 1.81\,\frac{mW}{mm^2}$ is sufficient for our application.

5.4 Challenges

a) The space above the sample plane is occupied by an imaging unit and in order to avoid Fresnel reflections we do not want a coaxial illumination. Therefore, the excitation beam of our projector forms a 45˚ angle with the sample plane. Hence, the beam spreads and increases in diameter as the beam is scanned through the whole FOV of the camera. This problem should be tackled so that the resolution remains as stable as possible at different locations of the sample plane.

b) The aperture of the Optotune mechanical scanning mirror is 15 mm, so the combination of the two converging lenses on both sides of the Fourier plane (that are used to focus the beam and then again collimate it) is chosen such that the parallel beam waist just fits into the aperture of 15 mm, so that the final through power output is maximum. Choosing the first lens with a larger focal length can result in an output beam of smaller diameter at the mirror. Hence, there is a trade-off between the optical path length of the system and the beam waist diameter at the scanning mirror. Larger optical path length results in larger space requirement.
Depending on the scanning mirror aperture dimension a telescopic lens system can also be built up to modulate the beam diameter at the scanning mirror.

c) Other components of the laboratory setup which are not related to the projector system reported here impose strict space constraints. The designed optical setup therefore should comply by these requirements.

5.5 Improving Irradiance Output

Homogenization of the spot diameter throughout the whole FOV area by introducing tilting and decentring of the optical components is one approach for increasing irradiance levels.

This method uses the Scheimpflug principle which states a geometric relationship between the orientation of the image plane, lens plane and plane of focus. Ideally, if the lens plane and the image plane lie parallel to each other, the plane of focus lies parallel to both the planes. When a lens plane is not parallel to the image plane, it is still possible to focus along the tilted image plane if the three planes, namely, the image plane, the lens plane and the plane of sharp focus converge along a single line, also termed as the “Scheimpflug Line” [5]

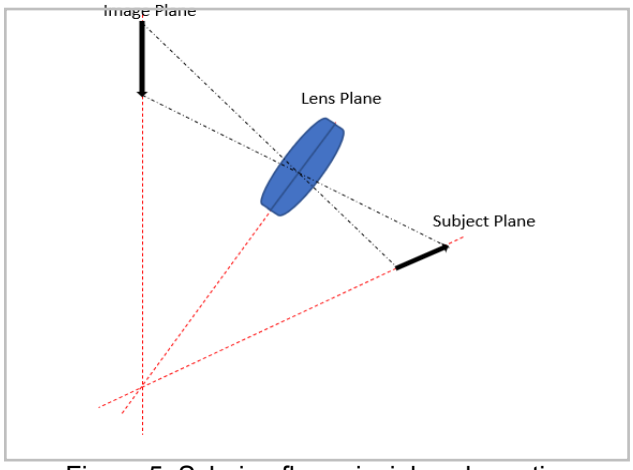

Figure 5: Scheimpflug principle schematic

Another approach is to decrease the spot radius by introducing an additional focusing lens as close as possible to the sample plane such that it does not interfere with the camera view.

In this paper, the third combination approach is applied. An additional focusing lens tilted at an angle of 10˚ with respect to the optical axis and at its focal length distance from the sample plane is placed. This maintains a high through power on the final sample surface and keeps the spot diameter constant as much as possible as the whole FOV is scanned.

5.6 Aperture Placement

To limit the spot diameter, a suitable aperture diameter is chosen. Depending on the filter transmission percentage, the aperture diameter is adjusted to modulate the final irradiance on the sample plane. The aperture positioning is also a crucial factor in the system designing. Optical spatial filtering is based on the Fourier transform property of a lens.

Low-pass filtering is a process which helps in improving the overall beam quality by allowing only the low spatial frequencies to pass through the system and blocking all higher frequencies.

The amplitude and phase information of an image can be altered by Fourier transforming the image using a lens, if an aperture is placed in the Fourier plane, followed by a second lens after the spatial frequency plane inverse Fourier transforms the amplitude transmission function of the filter convolved by the Fourier transform of the object function. [2]

Hence the Fourier plane is an ideal location for the aperture placement. Now by simulating the spot on the sample using different aperture radii, a suitable radius of 0.45 mm is chosen.

6 Simulation Results

6.1 Setup Layout and Optimisations

Considering all functional and constructional requirements, at first a 3D layout of the whole optical system using real lenses is created in the Zemax OpticStudio sequential mode using the light-source analysis module. Later, the system is re-modelled in the non-sequential mode to perform some stray light analysis and tolerancing.

The figure below shows the shaded model layout in Zemax, showing the light source (Kyocera SMD element), interference band-pass filter, aperture, scanning mechanical mirror and the camera field of view which corresponds to the sample plane in figure 5. The final focusing lens is inclined at an angle of 10˚ with respect to the normal to the optical axis to compensate for the beam-spreading effect on the sample plane as much as possible.

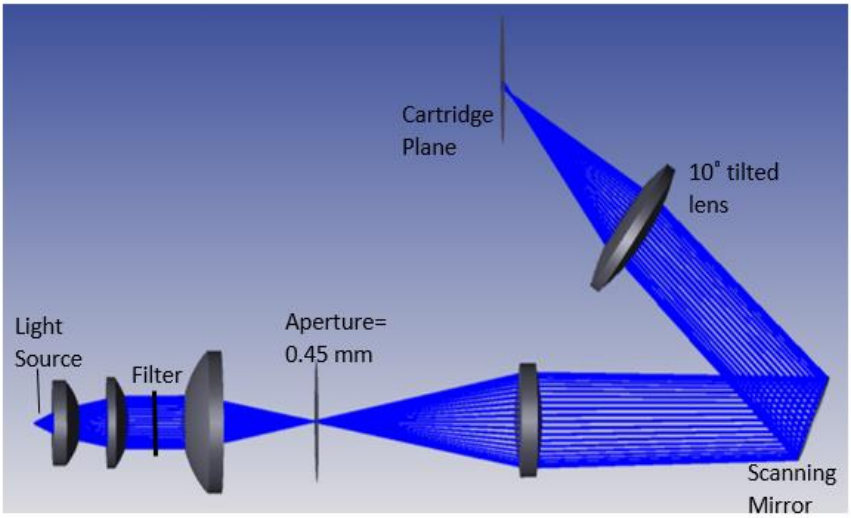

Figure 6: Zemax shaded model layout

As a next step, the required angular limits of the scanning mirror to access the FOV were calculated. Since the projection system consists of a scanning unit, the setup needs to be optimized for multiple configurations of the scanning beam on the sample plane.

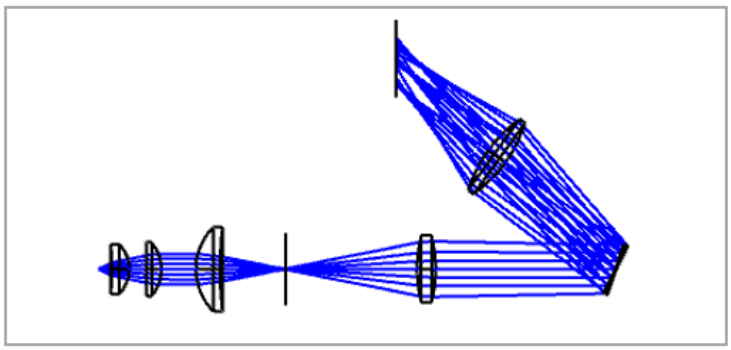

Figure 7: Multi-Configuration Optimisation Layout showing scanning beams at the extreme top, bottom, and centre of the FOV

6.2 Irradiance Profiles

The irradiance profiles of the source and the final detector plane are shown in the figures below and the spot radius is given by x-axis distance measured from the centre corresponding to the y-axis value of the peak irradiance $(I_o)/e^2$ which is the standard calculation for evaluating Gaussian beam waist diameter. The figures show how the spot size varies from being larger at the bottom of the sample plane and decreasing gradually to a small spot at the centre and again increasing at the top of the plane.

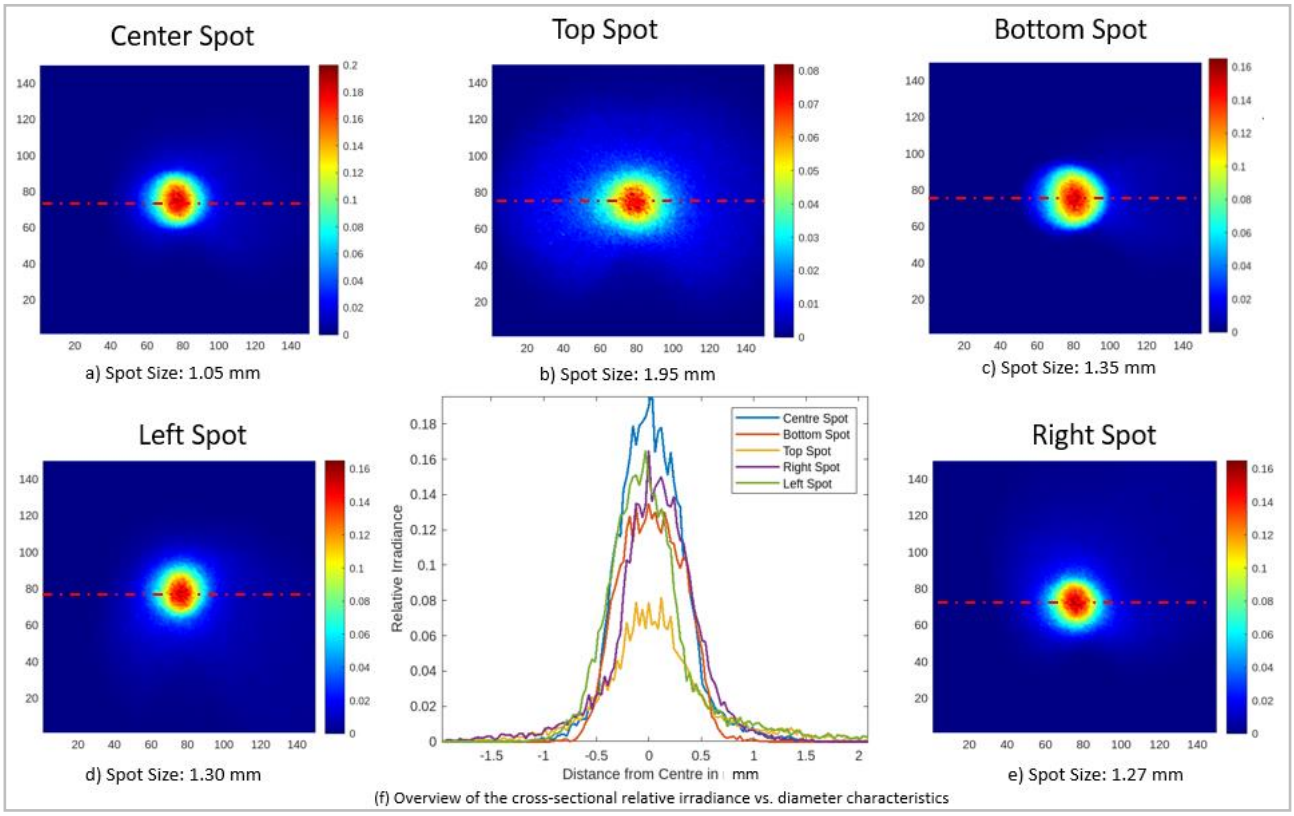

Figure 8:(a)-(e) Irradiance profiles of the final detector plane (sample plane) showing the respective spot diameters

The rate of variation of the spot diameter has been optimized using the Scheimpflug principle. Using this principle, an image plane which is not parallel to the lens plane can be focused.

A comparison between the two instances, one with the 10° tilted lens and the other with the untilted lens is shown in the figures below.

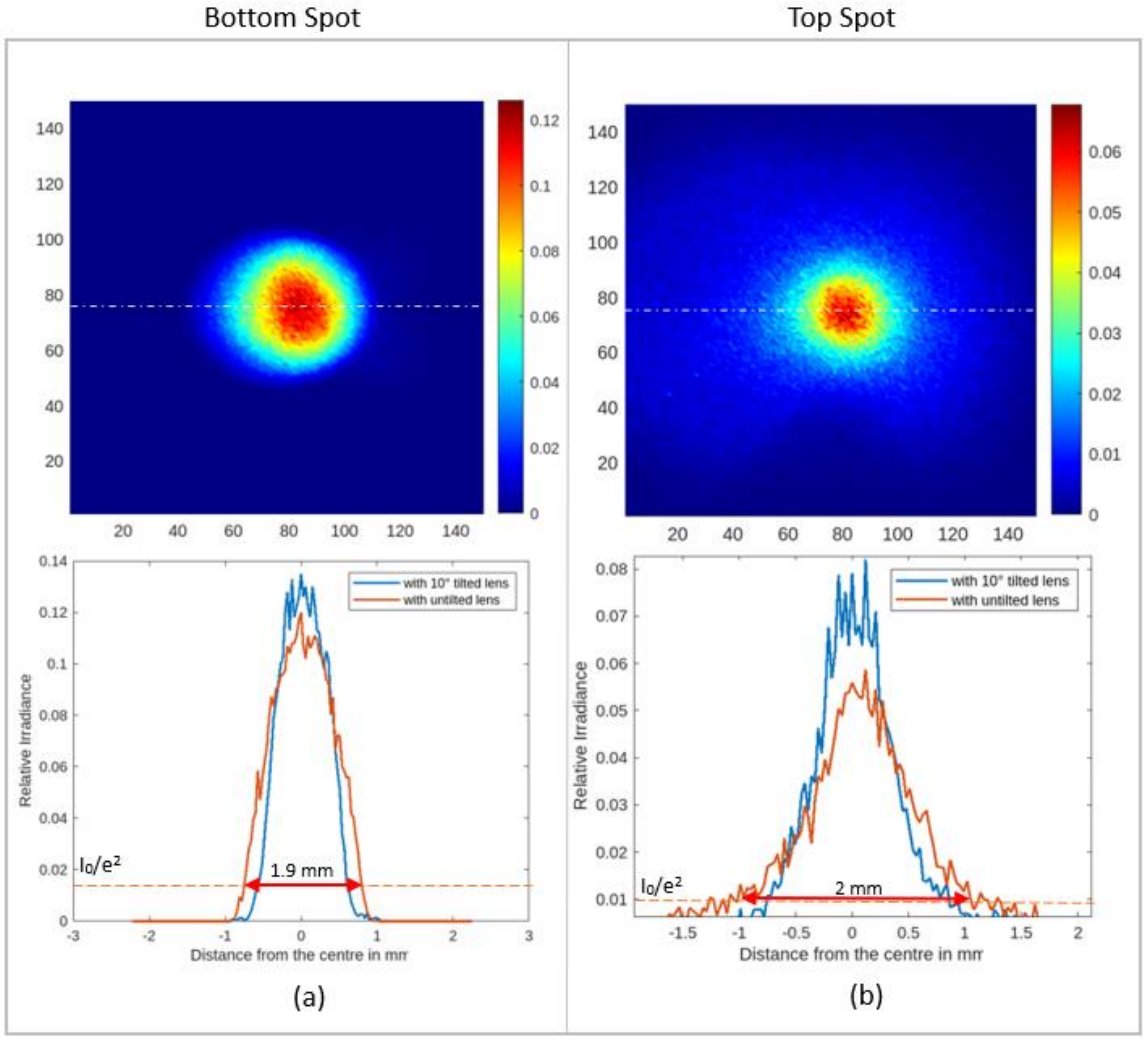

Figure 9: Irradiance profiles (setup with untilted lens) and comparison cross sectional irradiance vs. spot size characteristics showing the measured spot diameters of the bottom and top spots

It is evident from the graphs above that the spot size is larger comparatively at the top and the bottom part of the sample plane when an untilted focusing lens is used, for the same angle of inclination of the scanning mirror. Therefore, it is possible to scan the same FOV while maintaining a higher resolution using a tilted focusing lens.

One of the fundamental factors that might affect the result of the experimentation is the exact position of the light source. Therefore, it is observed that the irradiance output on the final detector plane varies by 1-1.5 mW (power on the final spot: 15.4 mW [4]) when the source position is displaced by ±100 µm. Apart from the source, some further tolerance analysis is performed on the setup components which helps to decide on the correct mounts for the experimental setup.

6.3 Mechanical Design

After the optical layout of the system with real components is finalized, it is necessary to create the mechanical setup as it should be built up in the lab for experimentation. Therefore, the setup is created in CAD software for clear and better evaluation.

Precise position controls are added to the light source and the adjustable aperture in order to maximize the power output of the system. As a heat sink for the source, a metal adapter plate is used. Figure 9 shows the CAD 3D layout of the optical setup. The available space is limited by the position of the detection unit which is not shown in figure 9. For the scanning system to function efficiently, the distance of the last focusing lens from the scanning mirror as well as the sample plane is extremely critical. The CAD model was constructed considering all the functional and mechanical requirements. The setup is built on a u-shaped customized breadboard and is made portable which allows for testing with or without the detector setup.

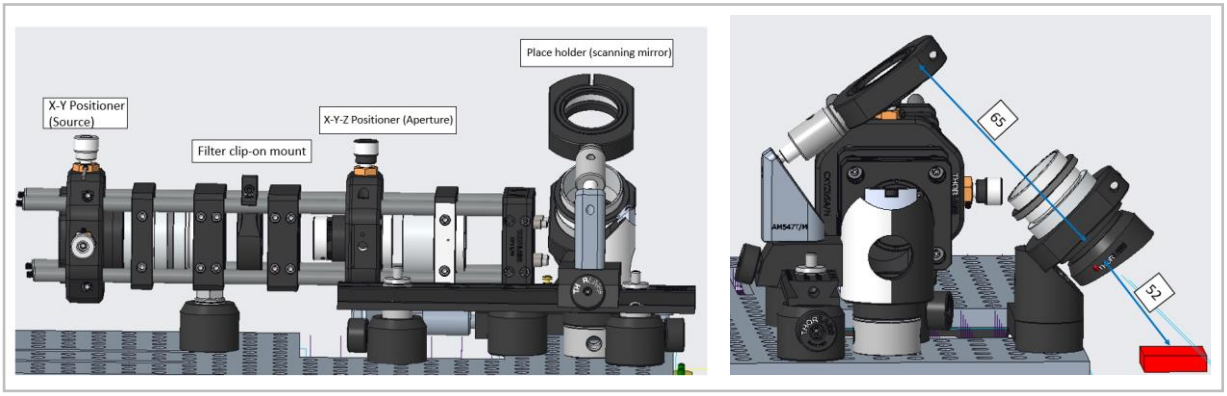

Figure 10: Front and side view of the mechanical setup in CAD 3D layout; In the right picture, the sample plane is given by the red cube and distances from the scanning mirror to the last focusing lens as well as from the last focussing lens to the sample plane are given in millimetre

7 Experimental Setup

The main goals of the lab experiment are to observe and study the spot sizes, irradiance and power levels obtained at the final sample plane as the projection system scans over the entire field of view.

As a first step, the prototype of the projection system is built in the lab following the mechanical design model that is previously built using CAD.

For measurement purposes, a camera with adjustable exposure time and focal length is mounted vertically above the sample plane in order to record images of the light spot at different chosen locations. The light source is operated at the optimum voltage rating of 8.7 V which corresponds to luminous flux of 500 lumens according to the datasheet [6]. The images of the spot were captured at the extreme top, bottom, right and left points of the sample plane.

The images are post processed to analyse the variation of spot size. At the start of camera measurement, a power meter is used to record the output power of the

projection system. In the images shown below, a band pass filter with centre wavelength of 530 nm is mounted. As a result, green light is obtained at the output.

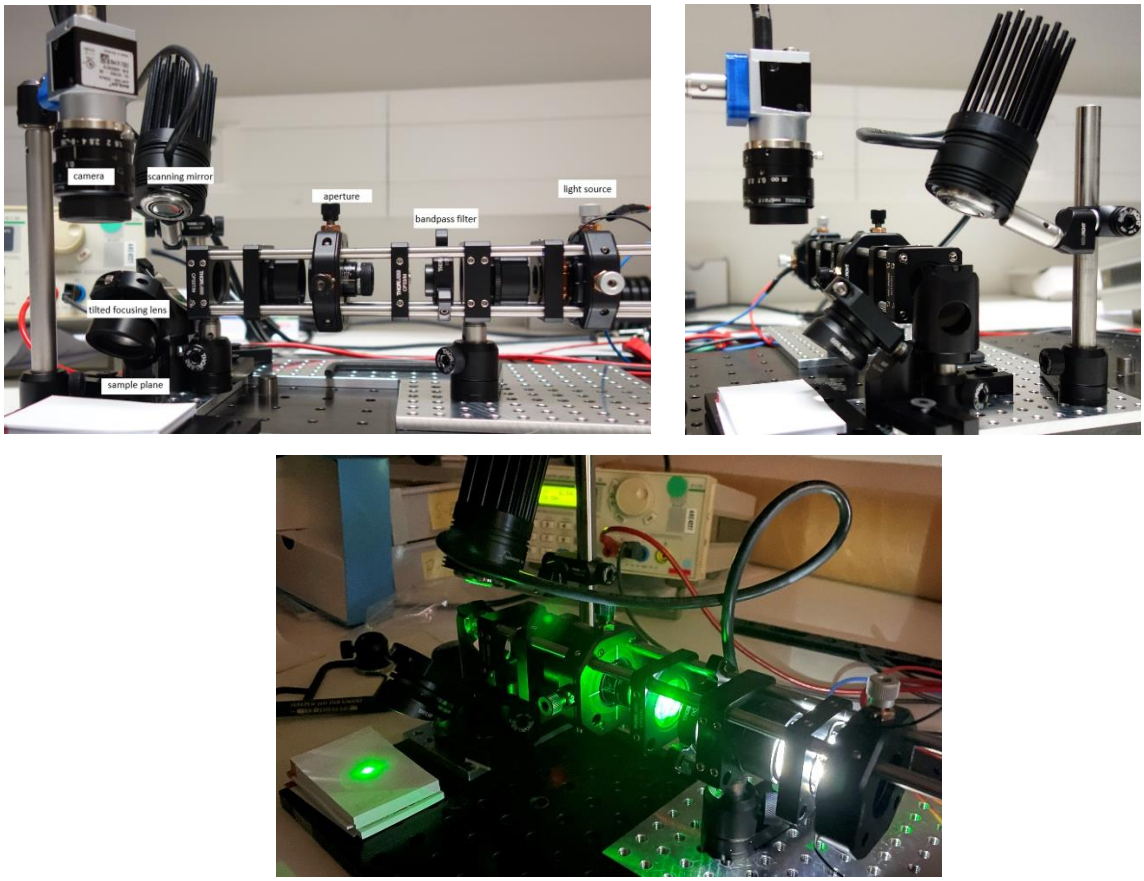

Figure 11: Lab Prototype Setup

8 Results and Discussion

To conclude the experimentation, it is necessary to compare the practical results with the simulations. From the camera image, the irradiance is obtained in the unit of bits. To make the comparison more apprehensible, the irradiance values are converted in the units of mW/mm^2. The calibration factor is calculated, considering the power meter reading in mW and the scaling factor between pixel to mm using a reference object of known dimensions. The grayscale intensity value obtained in 8 bits is then multiplied with this calibration factor. As a result of this, a direct comparison between the experiment and the simulation is achievable. The following section analyses this comparison.

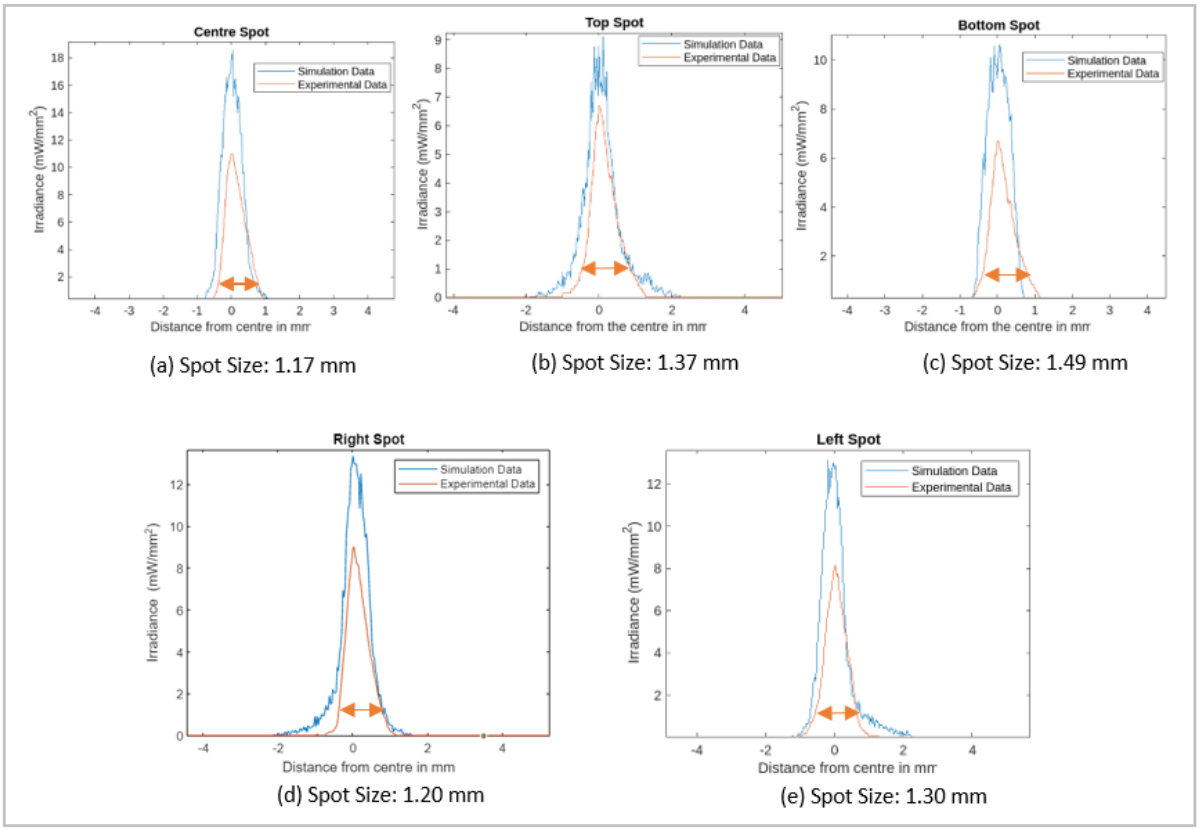

Figure 12: (a)-(e) Comparison plots showing variation between the cross-sectional irradiance value vs diameter for each of the centre, top, bottom, right, left spots as obtained from experimentation (orange curve) and Zemax simulations (blue curve) and the marked arrow corresponds to the experimental spot diameter measurements

It can be inferred from the comparison plots that the total output power in the experimental tests is lower than expected from the simulations. One explanation is the phenomenon of thermal quenching. When operating at the high power, a drop of luminous flux occurs at the output along with a rise in the source temperature. [1]

Apart from thermal degradation, the final efficiency of the system also depends on positioning tolerances and finer aligning of the vital components e.g., the light source, the aperture etc.

9 Conclusions

The first round of experimentation has been performed using the working prototype of the scanning projection system. The measured results comply closely with the simulation results except for a slight dip in the output power. In order to mitigate the problem, finer aligning adjustments of the crucial optical elements e.g., the aperture and the source are to be done to maximize the efficiency. However, more significant focus is on solving the issue of the thermal degradation of the source by using a suitable heat sink coupled with a cooling fan so that the source temperature can be controlled more effectively. For more accurate irradiance analysis, it is planned to use

a beam profiler for carrying out the measurements. In the future, the setup is to be integrated to a laboratory setup including a detection unit to perform a demo test.

10 Acknowledgement

The authors acknowledge the support of Navid Soltani, Marcus Liebler and Dieter Amesöder giving advice on critical components in the mechanical design of the flying-spot projection system.

11 References

[1] Hagemann V, Seidl A and Weidmann G, “Static Ceramic Phosphor Assemblies for high power high luminance SSL-light sources for digital projection and specialty lighting”, Light-Emitting Devices, Materials and Applications XXIV, 2020.

[2] Bahaa E. A. Saleh, Teich M.C., “Fundamentals of Photonics”, Wiley Blackwell, pp. 108-156, 2019.

[3] Optotune AG, “MR-E-2 Operation Manual”, March 2023.

[4] Kyocera, Kyocera SLD Laser LaserLight SMD 500 Technical Documentation, August 2022.

[5] Merklinger H. M., “Principles of View Camera Focus”, May 1996.

[6] Mouser, www.mouser.de/new/kyocera-avx/kyocera-sld-laserlight-smds/, Accessed 24 May 2023.